

Supporting Information

One-pot synthesis of N,S-doped pearl chain tube-loaded Ni₃S₂ composite materials for high-performance lithium-air batteries

Bohan An,^a Jiacheng Li,^a Xiaochao Wu,^a Wanqing Li,^{a,b,*} Yongliang Li,^a Lingna

Sun,^a Hongwei Mi ,^a Qianling Zhang,^a Chuanxin He,^a Xiangzhong Ren ^{a,*}

^a College of Chemistry and Environmental Engineering, Shenzhen University,

Guangdong 518060, PR China

^b Key Laboratory of Optoelectronic Devices and Systems of Ministry of Education

and Guangdong Province, College of Physics and Optoelectronic Engineering,

Shenzhen University, Shenzhen 518060, China

*Corresponding author.

E-mail address: renxz@szu.edu.cn, , liwanqing136@foxmail.com

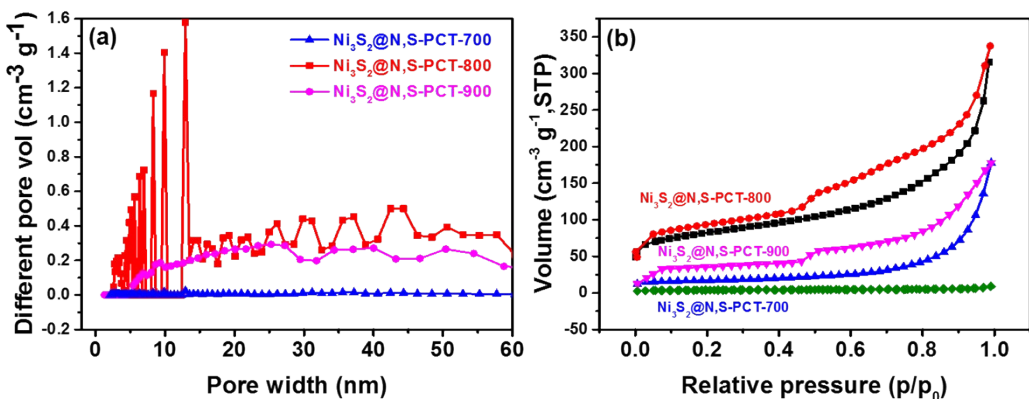


Figure S1 Under different temperature gradients (a) $\text{Ni}_3\text{S}_2@\text{N,S-PCT}$ of pore size distribution; (b) $\text{Ni}_3\text{S}_2@\text{N,S-PCT}$ of adsorption isotherm

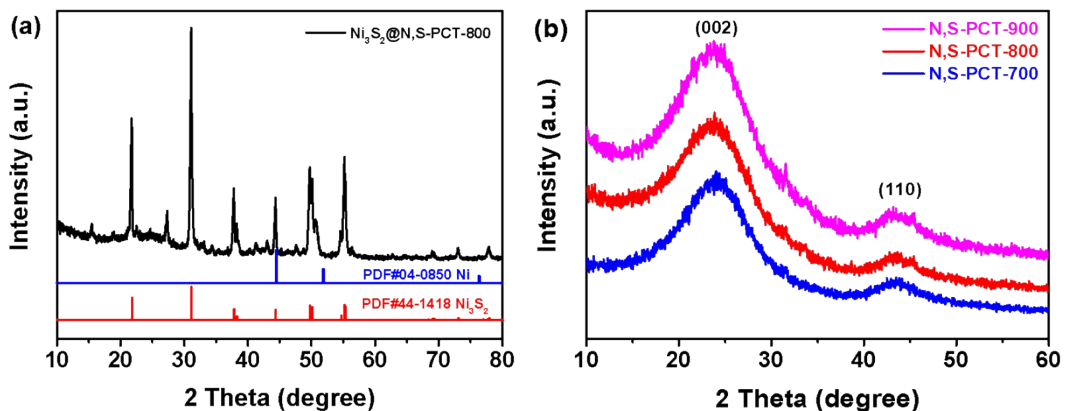


Figure S2 (a) XRD of material sample coated on carbon paper; (b) XRD of N,S-PCT at different temperatures

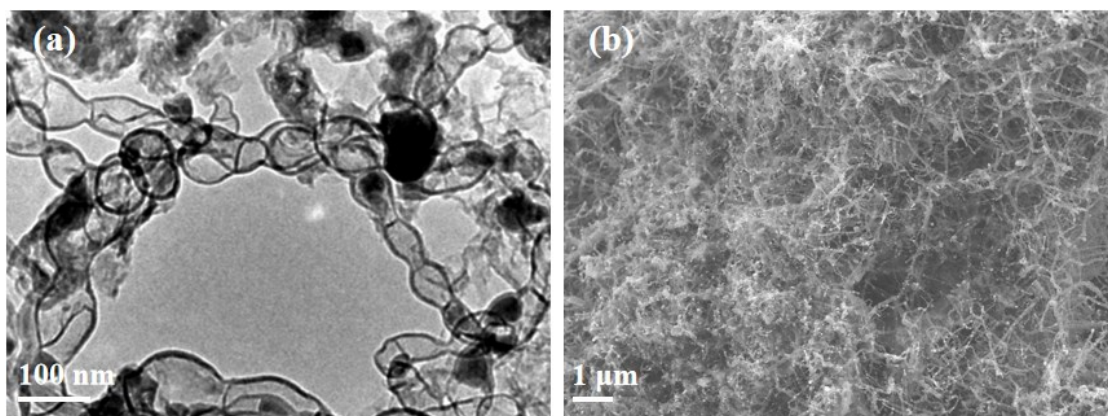


Figure S3 (a) Mapping the diameter of the carbon layer of N,S-PCTs; (b) the whole frame of $\text{Ni}_3\text{S}_2@\text{N,S-PCT-800}$

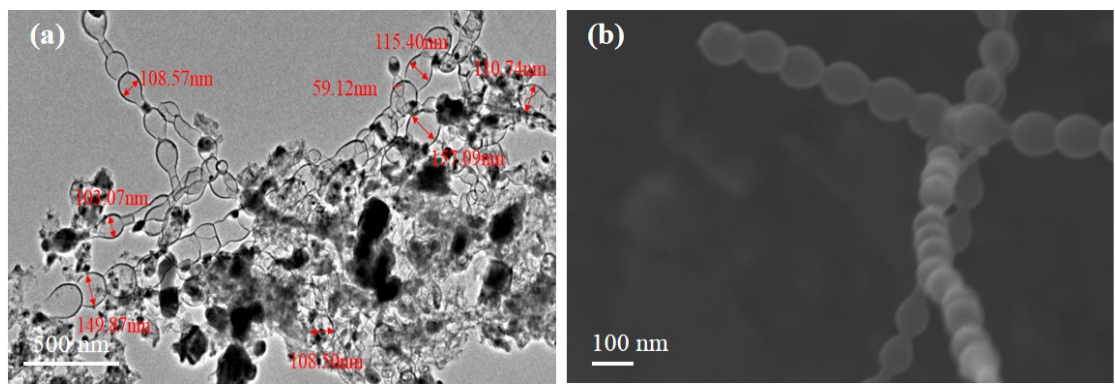


Figure S4 (a) Mapping the diameter of $\text{Ni}_3\text{S}_2@\text{N},\text{S-PCT-800}$; (b) SEM images of $\text{N},\text{S-PCT-800}$. The $\text{N},\text{S-PCT-800}$ obtained, the morphology of the carbon tube presents a pearl chain shape.

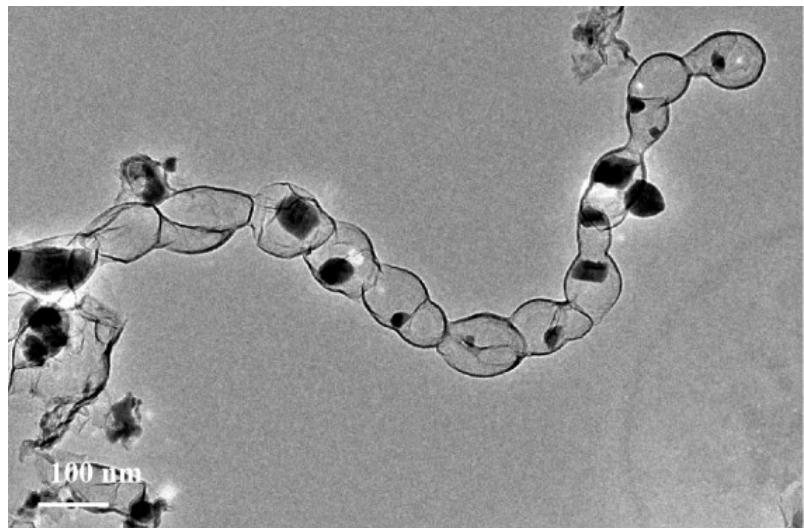


Figure S5. HRTEM images of $\text{Ni}_3\text{S}_2@\text{N},\text{S-PCT-800}$

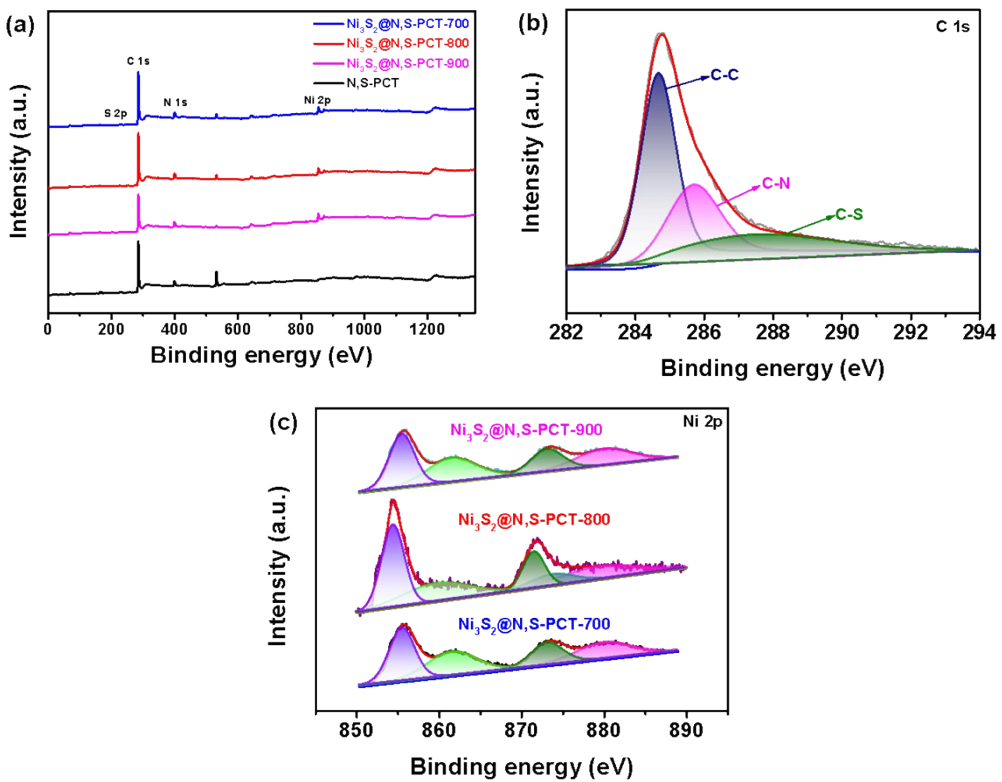


Figure S6 (a) XPS analysis of the samples in different temperatures; (b) XRD pattern of C 1s; (c) XRD pattern of Ni 2p from 700°C to 900°C

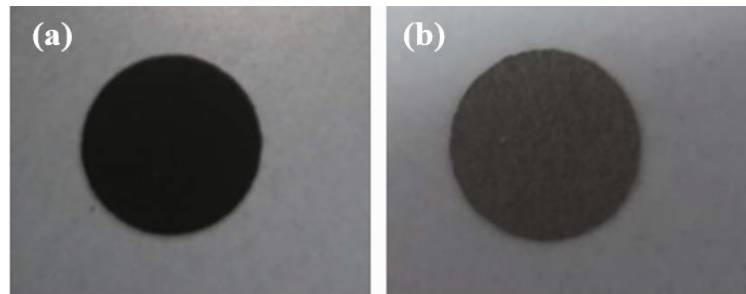


Figure S7. (a) loaded carbon paper (b) Original carbon paper

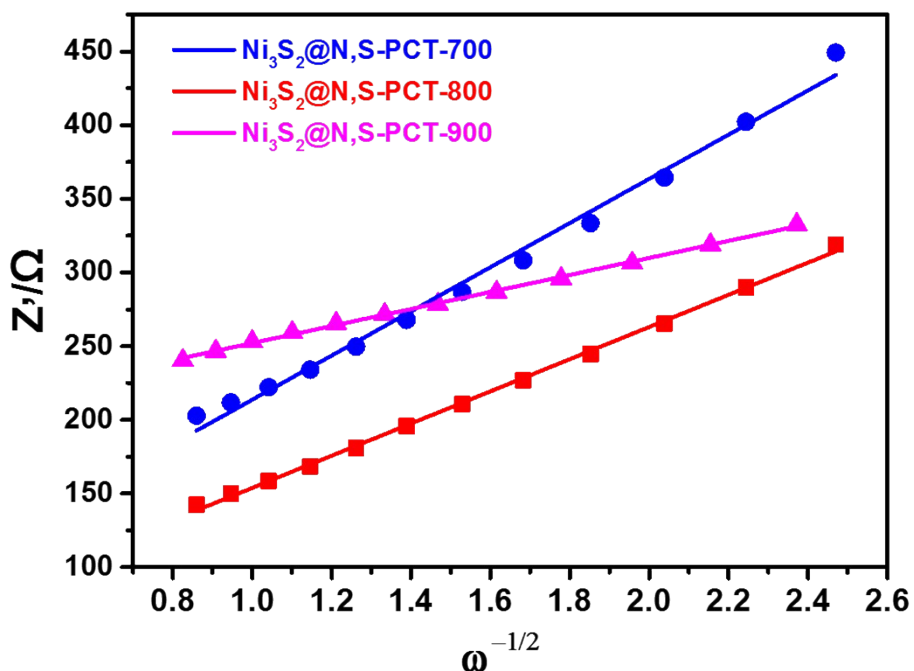


Figure S8. The relationship between Z' and $\omega^{-1/2}$ of O_2 electrode

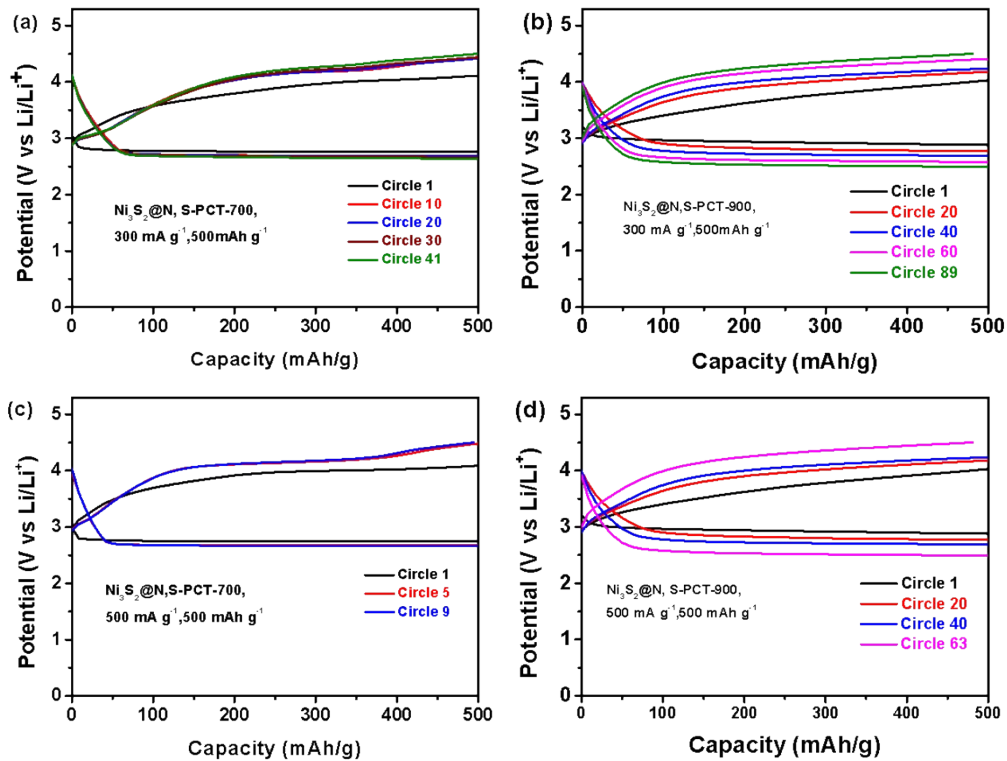


Figure S9. The discharge/charge profiles of (a) $\text{Ni}_3\text{S}_2@N,\text{S-PCT-700}$ and (b) $\text{Ni}_3\text{S}_2@N,\text{S-PCT-900}$, at a current density of 300 mA g^{-1} with a limited capacity of 500 mAh g^{-1} . The discharge/charge profiles of (c) $\text{Ni}_3\text{S}_2@N,\text{S-PCT-700}$ and (d) $\text{Ni}_3\text{S}_2@N,\text{S-PCT-900}$, at a current density of 500 mA g^{-1} with a limited capacity of 500 mAh g^{-1}

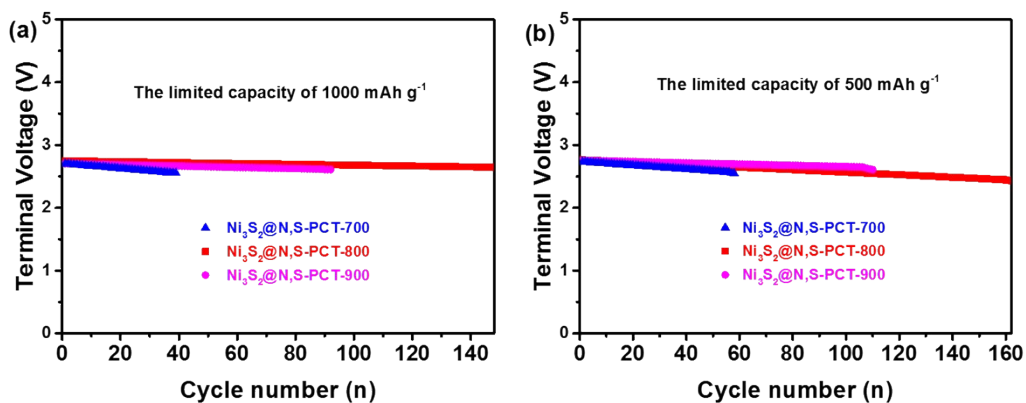


Figure S10. Cycle performance of the $\text{Ni}_3\text{S}_2@N,\text{S-PCT-900}$, $\text{Ni}_3\text{S}_2@N,\text{S-PCT-800}$ and $\text{Ni}_3\text{S}_2@N,\text{S-PCT-700}$ electrodes (a) at current density of 450 mA g^{-1} with limited capacity of 1000 mAh g^{-1} (b) at current density of 500 mA g^{-1} with limited capacity of 500 mAh g^{-1}

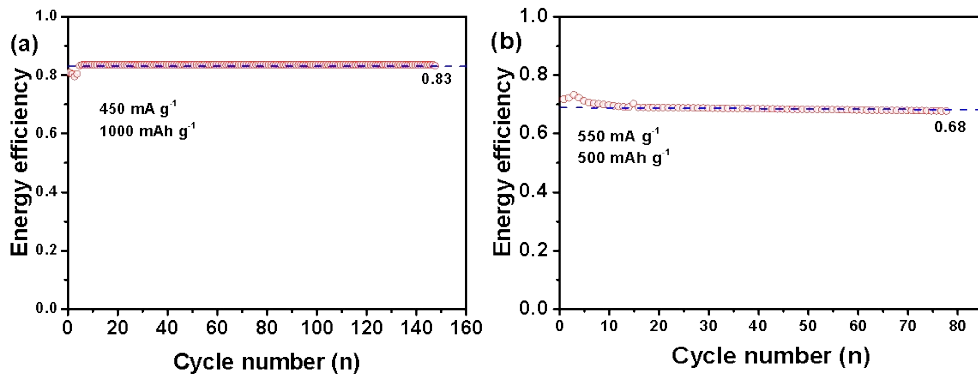


Figure S11. The cycle efficiency of $\text{Ni}_3\text{S}_2@\text{N},\text{S}-\text{PCT-800}$ (a) the current density is 450 mA g^{-1} and the limited capacity is 1000 mAh g^{-1} (b) the current density is 550 mA g^{-1} and the limited capacity is 500 mAh g^{-1}

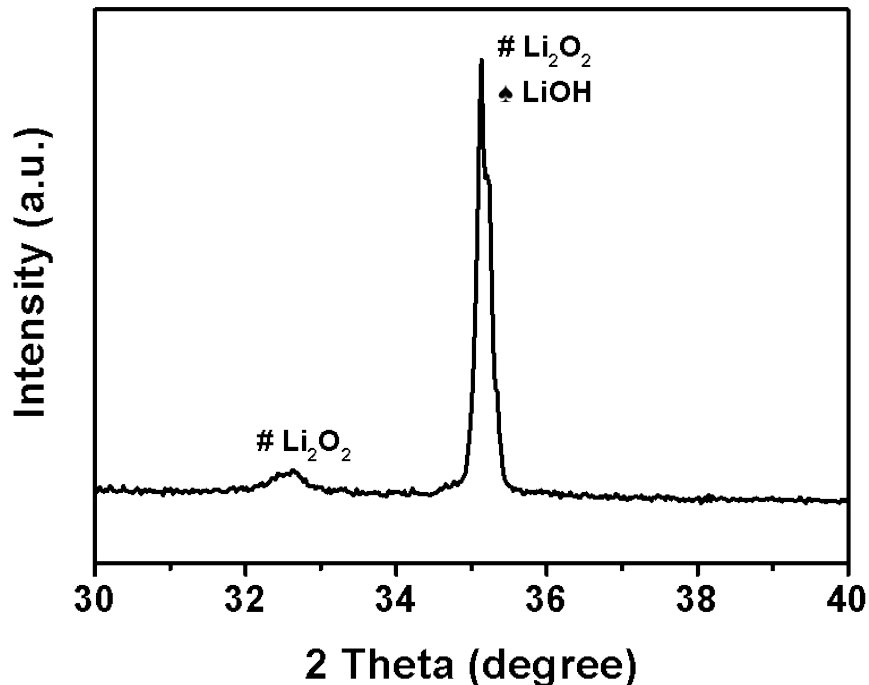


Figure S12. XRD analysis chart of discharge products in a certain range.

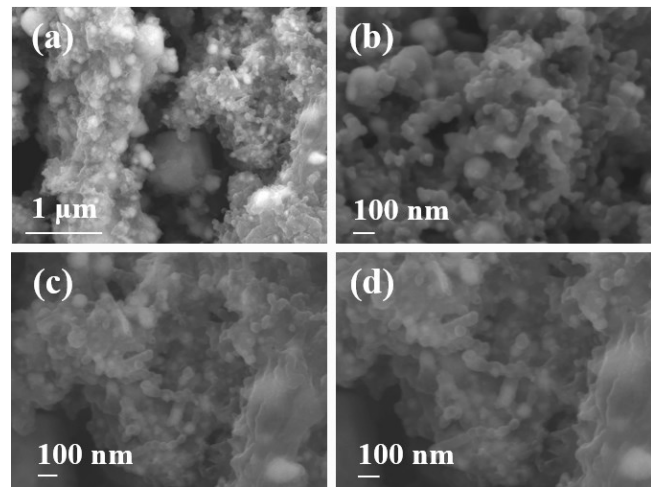


Figure S13. SEM image of materials after circulation in different positions (a)
Magnification is 20,000; (b) Magnification is 50,000; (a) Magnification is 40,000; (a)
Magnification is 50,000

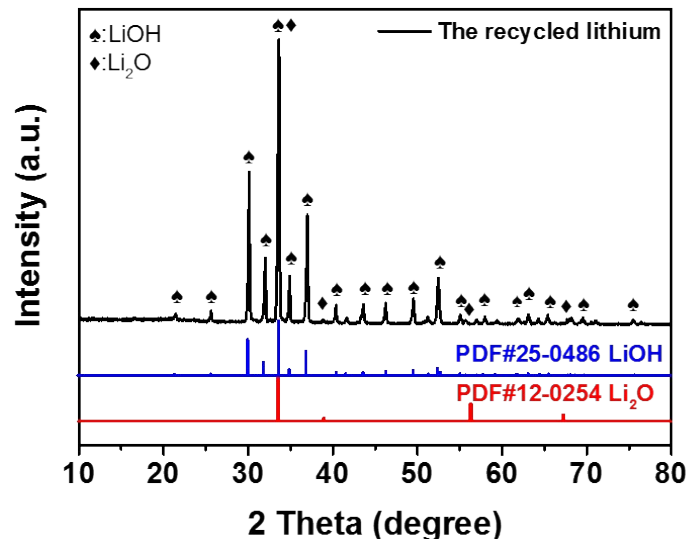


Figure S14. XRD patterns of the recycled lithium

Table S1. Elemental content percentage measured by XPS

| Sample name | Ni (at. %) | O (at. %) | C (at. %) | N (at. %) | S (at. %) |
|---|---------------|--------------|--------------|--------------|--------------|
| Ni ₃ S ₂ @N,S-PCT-900 | 1.8 | 11.06 | 76.51 | 7.73 | 2.91 |
| Ni ₃ S ₂ @N,S-PCT-800 | 3.24 | 2.98 | 81.95 | 10.63 | 1.34 |
| Ni ₃ S ₂ @N,S-PCT-700 | 1.88 | 4 | 83.96 | 9.13 | 1.03 |
| N,S-PCT | 0.53 | 2.7 | 85.67 | 10.07 | 1.17 |

Table S2. Comparison of Li-O₂ battery properties of Ni₃S₂@N,S-PCT-800 cathode with those of representative state-of-the-art cathodes reported in literature.

| Catalysts | Current Density (mA g ⁻¹) | Overpotention (V) | Cycling Performance (Cycles/Limited Capacity) | First Discharge Capacity (mAh g ⁻¹) | Ref. |
|--|--|----------------------|--|--|------------------|
| 2D Co ₃ S ₄ nanosheets | 100 | 0.92 | 25/500 | 5917 | 1 |
| Ni ₃ S ₂ | 200 | 1.29 | 50/500 | 7478 | 2 |
| MoS ₂ nanoflakes | 100 | ≥1.0 | 50/500 | 1250 | 3 |
| Ni ₃ S ₂ /PBSC NFs | 100 | 0.68 | 120/500 | 12874 | 4 |
| Co ₉ S ₈ | 100 | 1.37 | 100/500 | 3500 | 5 |
| MoS _x /HRG | 0.05 | 1.5 | 30/500 | 6678 | 6 |
| TiC/MWNTs-Ru | 250 | 0.49 | 90/1000 | 3841 | 7 |
| GDP-Mo ₂ C@NCF | 100 | 1.2 | 100/1000 | 7437 | 8 |
| NCS/S-3DPG | 150 | 1.38 | 102/1000 | 14,173 | 9 |
| Co ₂ P/Ru/CNT | 100 | 1.22 | 120/1000 | 12 800 | 10 |
| Ni₃S₂@N,S-PCT-800 | 450 | 1.45 | 148/1000 | 16733.7 | This work |

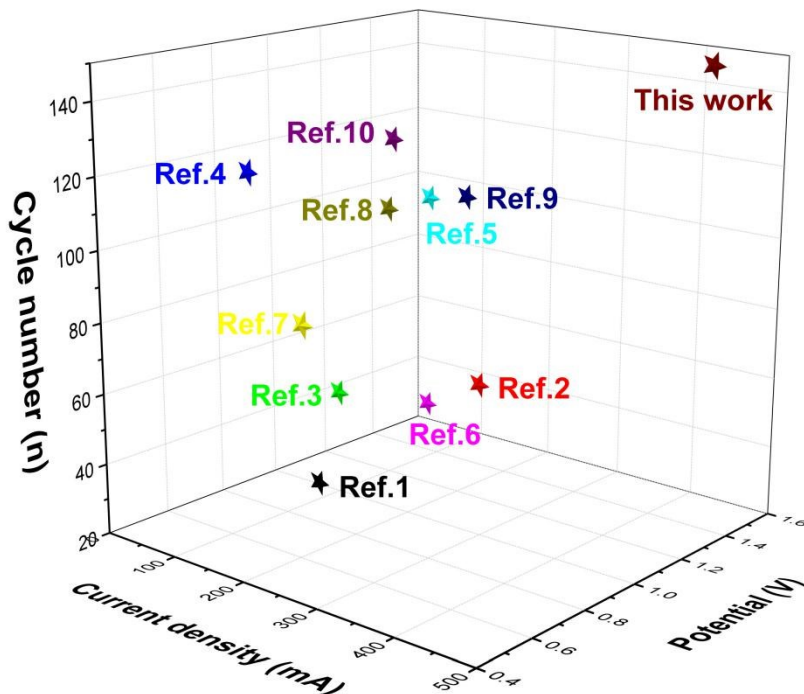


Figure S12 Lithium-air battery performance of different types of cathode materials

REFERENCE

1. P. Sennu, M. Christy, V. Aravindan, Y.-G. Lee, K. S. Nahm and Y.-S. Lee, *Chem. Mater.*, 2015, **27**, 5726-5735.
2. Q. Wang, X. Wang and H. He, *J. Power Sources*, 2020, **448**, 227397.
3. M. Asadi, B. Kumar, C. Liu, P. Phillips, P. Yasaei, A. Behranginia, P. Zapol, R. F. Klie, L. A. Curtiss and A. Salehi-Khojin, *ACS Nano*, 2016, **10**, 2167-2175.
4. Z. Zhang, K. Tan, Y. Gong, H. Wang, R. Wang, L. Zhao and B. He, *J. Power Sources*, 2019, **437**, 226908.
5. G. Wang, Y. Li, L. Shi, R. Qian and Z. Wen, *Chem. Eng. J.*, 2020, **396**, 125228.
6. L. Li, C. Chen, J. Su, P. Kuang, C. Zhang, Y. Yao, T. Huang and A. Yu, *J. Mater. Chem. A*, 2016, **4**, 10986-10991.
7. C.-S. Yang, Z. Sun, Z. Cui, F.-L. Jiang, J.-W. Deng and T. Zhang, *Energy Storage Mater.*, 2020, **30**, 59-66.
8. Z. Sun, B. Li, C. Feng, X. Cao, X. Zheng, K. Zeng, C. Jin, X. Wu, D. Dai and R. Yang, *J. Mater. Chem. A*, 2020, **8**, 14815-14821.
9. S. Hyun, B. Son, H. Kim, J. Sanetuntikul and S. Shanmugam, *Appl. Catal. B*, 2020, **263**, 118283.
10. P. Wang, C. Li, S. Dong, X. Ge, P. Zhang, X. Miao, Z. Zhang, C. Wang and L. Yin, *Small*, 2019, **15**, 1900001.